

Computational Model Predictions of Suspension Rheology: Comparison to Experiment

N. S. Martys¹, C.F. Ferraris¹, V. Gupta², J.H. Cheung²,
J. G. Hagedorn¹, A. P. Peskin¹, E. J. Garboczi¹

¹*National Institute of Standard and Technology, Gaithersburg, MD, USA ;*

²*W.R. Grace & Co.-Conn., 62 Whittemore Ave., Cambridge, MA, USA*

Predicting the rheological properties of fresh concrete, mortars, and cement paste from first principles remains a great challenge. While progress has been made in modeling the rheological properties of idealized hard sphere-like suspensions, there is little in the way of theoretical predictions and experimental data for suspensions composed of random shaped particles like those found in cement-based materials. In this paper, results will be presented of a study comparing computational model predictions to experimental measurements of the rheological properties of various suspensions. The model incorporates the particle size distribution as well as the shape of particles as determined from X-ray microtomography. The experimental rheological properties will be based on measurements using co-axial rheometers and various materials that could potentially be used as reference materials.

1 Introduction

Predicting the rheological properties of suspensions like fresh cement paste or concrete remains a great challenge. Some of the complicating factors in modeling such systems include the broad size and shape distribution of the cement, sand and coarse aggregates. Another challenge is the fact that most rheometers need to be modified to accommodate the larger particles. These modifications lead to rheometers with geometries that do not allow for an analytical solution of the flow pattern, making it extremely difficult to determine rheological parameters, such as yield stress and plastic viscosity, in fundamental units. Therefore, a combination of flow simulation in complicated geometries, particulate reference materials and modified rheometers need to be used to characterize suspensions.

To develop a realistic model, several considerations need to be taken into account: shape of the particles, spread of the particle size distribution (mono-size, or wide range of sizes), and the time evolution of the particle shape due to chemical interaction between the particles and the medium (e.g., cement hydration). Traditionally, most simulation models have relied on using idealized mono-size hard sphere suspensions. Such models are useful for developing a framework for understanding different phenomena and in capturing general trends, but these models lack predictive capability because measurements are generally made on far more complicated systems.

In this paper, some recent advances in modeling suspensions with realistic shaped particles are described and simulation results are compared with rheological measurements of suspensions composed of similarly-shaped particles.

2 Simulation Model

The simulation of suspension flow is based on a mesoscopic model of complex fluids called “dissipative particle dynamics” (DPD) [1] that blends together cellular automata ideas with molecular dynamics methods. A detailed discussion of this approach is beyond the scope of this paper; however, most of this computational approach is described in a paper by Martys [2]. The original DPD algorithm utilized symmetry properties such as conservation of mass, momentum and Galilean invariance to construct a set of equations for updating the position of particles, which can be thought of as representing clusters of molecules or “lumps” of fluid. Later modifications to the DPD algorithm resulted in a more rigorous formulation and improved numerical accuracy [2]. An algorithm for modeling the motion of arbitrary shaped objects subject to hydrodynamic interactions by DPD was suggested by Koelman and Hoogerbrugge (KH) [3, 4]. The rigid body is approximated by “freezing” together a set of randomly placed particles where the solid inclusion is located and updating their position

according to the Euler equations. Another important modification to the model was to account for the short range hydrodynamic interaction between the particles. This is achieved by adding lubrication forces between the particles and taking into account the local curvature of the particles [5].

The realistic shapes of particles are obtained by X-ray tomography and a spherical harmonics analysis is used to mathematically obtain the particle shape from the data collected [6]. From the spherical harmonic representation, the surface normals, principal axes and local curvatures are determined. This information is used to determine the lubrication forces between particles. In this study, eight different particle shapes were used. Some were somewhat rounded and others more angular (Figure 1). The particles varied by about a factor of three in size and aspect ratio.

To create a suspension, particles were randomly placed in a cubic computational cell. The number of particles was selected to obtain different volume fractions similar to the experimental data. A shear boundary condition was imposed and the stress tensor was calculated from the interparticle interactions. The viscosity of the suspension was then determined by dividing the shear stress by the shear rate.

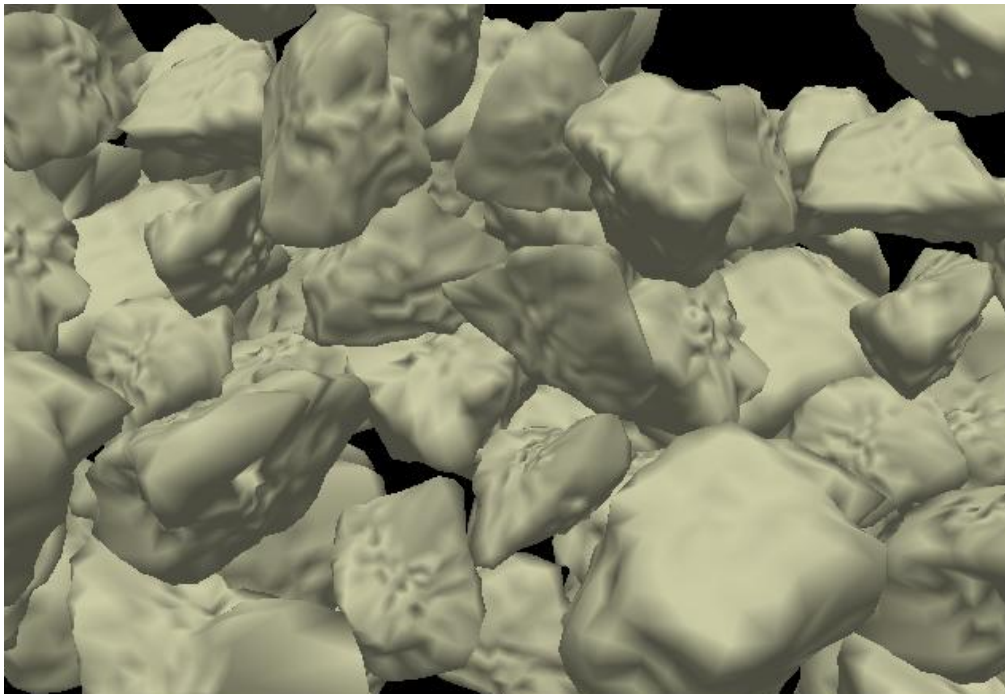


Figure 1: Random particle shapes derived from X-ray tomography of cement particles

3 Materials

The particles selected were either spherical or crushed/irregular shape. The medium selection was based on two criteria: 1) Newtonian liquid; and 2) non-reactivity with the particles. Table 1 shows the matrix of materials used.

The material used included a slag, a fly ash, three different oils and a solution of water with a high range water reducing admixture (HRWRA). The HRWRA was a commercially available polycarboxylate ether.

Table 1: Materials selection

		Particles	
		Slag (S)	Fly Ash (FA)
Medium	Various oils	X	X
	Water +HRWRA	X	

The particle size distribution of the slag is shown in Figure 2. Slag S1 is a poly-disperse slag. S2 represents the sieved portion of the slag, which has a narrow size distribution. For slag S1, the surface area and mean size as determined by laser light scattering were $613 \text{ m}^2/\text{kg}$ and $7.7 \text{ }\mu\text{m}$, respectively. The density was $2920 \text{ kg}/\text{m}^3$. For slag S2, the mean size was $65 \text{ }\mu\text{m}$, with a range between $29 \text{ }\mu\text{m}$ and $190 \text{ }\mu\text{m}$. The surface area was $36.9 \text{ m}^2/\text{kg}$.

The fly ash particle size distribution is also shown in Figure 2. The mean particle size was $20 \text{ }\mu\text{m}$, the surface area was $457 \text{ m}^2/\text{kg}$, and the density was $3040 \text{ kg}/\text{m}^3$.

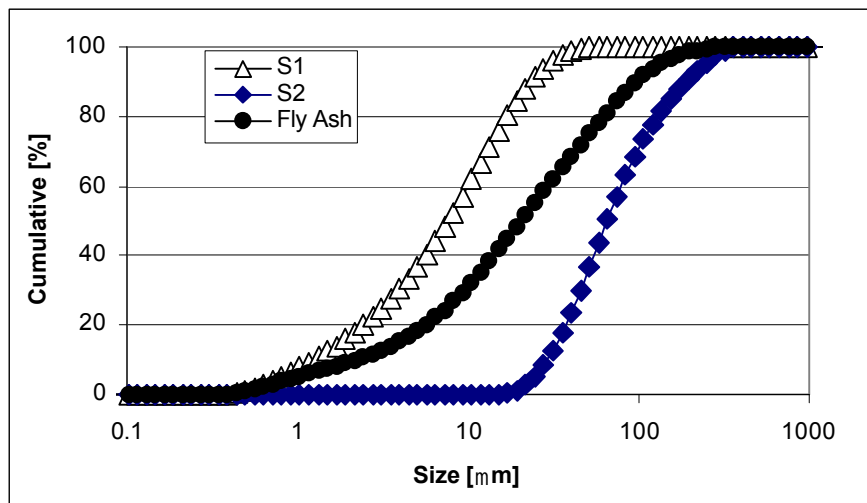


Figure 2: Particle size distribution (PSD) for the slag and the fly ash

Standard oils (Oil B and C) used for calibration of fluid rheometers and an oil that is used for preparing the mixture to calibrate flow tables (Oil A) were used. Table 3 shows the properties of the oils.

Table 3: Oil properties

	Oil A Flow Table oil	Oil B RT5000	Oil C RT1000
Viscosity at 23 °C [Pa·s]	0.076 ± 0.008	5.40 ± 0.12	1.10 ± 0.002
Density at 23 °C [kg/m ³]	866 ± 20	970*	970*

Note: * as provided by the manufacturer

4 Experimental Set-up

4.1 Suspension preparation

The samples were prepared using different methods as appropriate for the raw materials.

- ◆ The oils and FA or slags were initially mixed using a high shear impeller,; then they were hand mixed before each measurement.
- ◆ The slag suspensions were prepared using a mixer with a rotation speed of 41.8 rad/s (400 rpm) following a 4 min mixing cycle. The HRWRA and water were added to the slag and mixed for 30 s in a container. Then mixing was stopped for 15 s to allow for scraping of materials off the sides of the container. Mixing was resumed for another 75 s. At the end of 2 min, the scraping action was repeated for 15 s and the suspension was allowed to rest for 45 s. After that, mixing was resumed for another minute.

All suspensions, using any of the combinations in Table 1, were prepared at several different solid volume fractions varying from 20 % to 60 % depending on the materials.

4.2 Rheological Measurements

Rheology measurements were performed using two different co-axial viscometer geometries, Types G and N. Table 4 gives their geometrical specifications.

In all cases, the rheometers were used in a shear controlled manner. For the parallel plate and the coaxial N rheometer, the shear rates were increased and then decreased while measuring the shear stress. The descending data were linearly fit and the slope was calculated. In a pure Newtonian fluid, the slope is the viscosity but, in this case, a better fit was obtained with Bingham equation, so that the slope was really the plastic viscosity. However, for the coaxial G rheometer, the viscosity measured at

a preselected shear rate of 80 s^{-1} was reported as the viscosity. This is the apparent viscosity.

For the coaxial N rheometer, 10 measurements were taken with a 20 s integration time. For the coaxial G rheometer, 20 measurements, with a 2 min integration time, were performed to generate the viscosity curve. The viscosity reported is the ratio of shear stress to shear rate at a shear rate of 80 s^{-1} .

Table 4: Rheometer geometrical specifications

	Coaxial G	Coaxial N
Gap between shear planes [mm]	1.25	2.5
Diameters outer container [mm]	27.5	43
Diameter of inner bob [mm]	25	38
Type of surface of shearing plates	Sand blasted	Smooth
Range of shear rates	1 s^{-1} to 200 s^{-1}	1 s^{-1} to 45 s^{-1}
Model used to calculate viscosity	Ratio shear stress/shear rate at 80 s^{-1}	Bingham on descending curve

4.3 Relative viscosity

The concept of relative viscosity will be used here to compare simulation and experimental data [7]. The relative viscosity is defined as the ratio between the viscosity of the suspension and the viscosity of the medium. Therefore, two suspensions with the same concentration of particles and similar particle shape (round or angular) should have similar relative viscosity values. Comparison between measured data and simulation data then becomes possible.

5. Results

The data obtained for all measurements and all simulations are shown in Figure 3. The coefficient of variation (COV), for slag S1 or S2, calculated from three suspension duplicate measurements was 10 %. The COV was also 10 % for the data obtained with the other materials as estimated from measurements done with the same instruments [8]

To use the concept of plastic viscosity, the measurement of the medium is paramount. An error in this value can cause relative viscosities that are too high or too low. The measurements of the oil are standard and are reported in Table 3. On the other hand, the viscosity measurements of the aqueous solution used for slag S1 required more careful measurements. The medium was a 10 % by mass fraction solution of the HRWRA in water and gave a viscosity of 0.0025 Pa·s (7 % COV obtained from duplicate measurements).

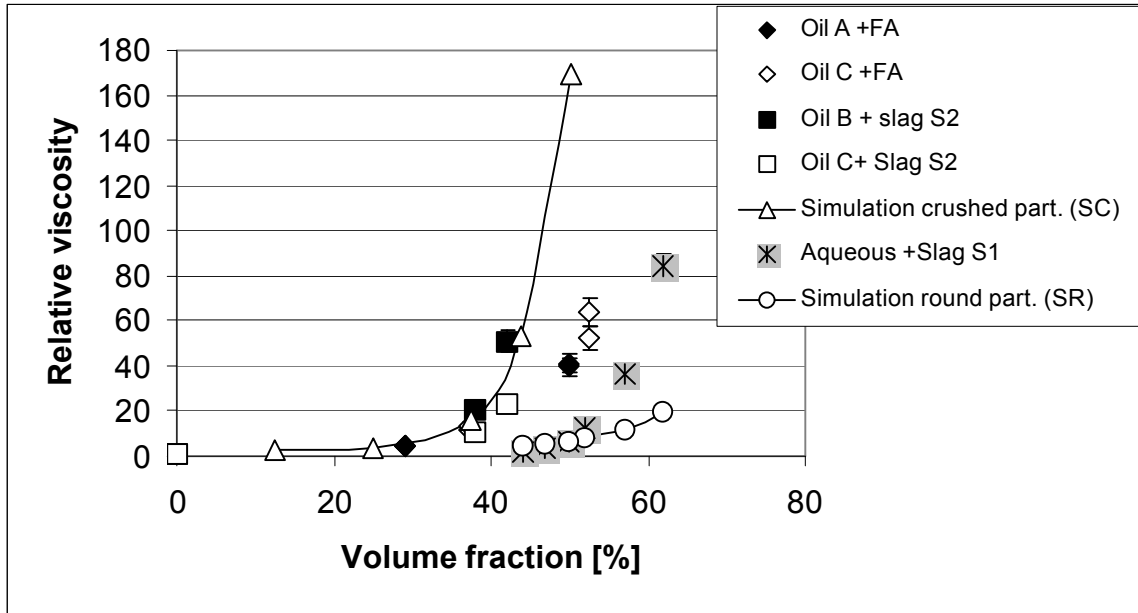


Figure 3: Relative viscosity versus volume fraction for all materials used. The error bars correspond to the COV error estimated from replicate measurements (if not visible, the error bars are smaller than the symbol).

6 Discussion and Conclusion

Figure 3 shows all the data obtained from simulations and experiments. The two simulations are: 1) wide particle size distribution of spherical particles (SR), and 2) narrower particle size distribution of crushed particles as shown in Figure 1 (SC). It appears that all the experimental results could be roughly separated into three groups: 1) the data obtained with the S1 slag, 2) the data obtained with the slag S2 and 3) the data obtained with fly ash (FA).

It is interesting to note that the simulation SR matches the data for S1 for volume fraction lower than 50 %. This implies that the particle size distribution has a larger effect than the shape. In other words, the slag S1 particles have a crushed shape (as in Figure 1) and a wide size distribution yet they match the simulation obtained with the wide distribution and spherical particles for volume fraction below 50%. For a

volume fraction above 50 %, for slag S1, the experimental data increases more rapidly than the simulation data (SR) from Figure 3. At these high volume fractions, the shape of particles plays a very large role in the viscosity. The flattened sides of the particles have a tendency to push against each other making it difficult for the particles to flow pass each other. Therefore, the system has a tendency to temporarily lock or jam. This phenomenon is not accounted for in the simulation SR. On the other hand, the slag S2 matches simulation SC because the shape and the particle size distribution are both taken into account in the simulation.

The shape of the fly ash was considered to be spherical, while slag S2 was crushed. The results for fly ash are in between the two simulations because the particles are spherical while having a particle size distribution between the slags (Figure 2). It is conceivable that the fly ash particles could have agglomerated or are not well dispersed in the oil. This will have a tendency to increase the relative viscosity from a well dispersed system as considered in simulation SR. The spherical shape will reduce the relative viscosity from the crushed shape considered in simulation SC.

We have shown that by accounting for size distribution of particles and shape, we can more closely correlate measurement results with simulation models. For the lower volume fraction, the shape does not appear to have a strong influence on the data. This research could serve as a basis for establishing a reference material to be used both for validation of models and for calibration of rheometers of non-conventional geometries.

7 Acknowledgements

The author would like to thank the VCCTL™ Consortium for its financial support. We are grateful to Barry Descheneaux (Holcim) for providing the slag, and to Dan Ratjer (WR Grace), John Winpigler (NIST) and Max Peltz (NIST) for performing the experimental measurements. Dr. Jeff Bullard should be thanked for reviewing the paper and providing useful comments.

8 References

- [1] R.D. Groot and P.B. Warren, "Dissipative particle dynamics: Bridging the gap between atomistic and mesoscopic simulation", J. Chem Phys. 107 (1997) 4423-4435
- [2] N.S. Martys, "Study of a dissipative particle dynamics based approach for modeling suspension," J. Rheol. 49 (2005) 401-424

- [3] P.J. Hoogerbrugge, and J.M.V.A Koelman, "Simulating microscopic hydrodynamic phenomena with Dissipative Particle Dynamics", *Europhys. Lett.* 19 (1992) 155-160
- [4] J.M.V.A. Koelman, P.J. Hoogerbrugge, "Dynamic simulations of hard-sphere suspensions under steady shear", *Europhys. Lett.* , 21 (1993) 363-368
- [5] R.G. Cox, "The motion of suspended particles almost in contact," *Int. J. Multiphase Flow* 1(2) (1974) 343-371
- [6] E.J. Garboczi, "Three-dimensional mathematical analysis of particle shape using X-Ray tomography and spherical harmonics: Application to aggregates used in concrete," *Cem and Concr Res*, 32(10) (2002) 1621-1638
- [7] C. F. Ferraris, N. S. Martys, "Relating fresh concrete viscosity measurements from different rheometers", *J. Res. Natl. Inst. Stand. Technol.* 108(3) (2003) 229 -234
- [8] C. F. Ferraris, "Measurement of the rheological properties of cement paste: a new approach", *Int. RILEM Conf. "The role of Admixtures in High Performance Concrete"*, ed. by J.G. Cabrera and R. Rivera-Villareal, Monterrey (Mexico) March (1999) 333-342